

## Monte Carlo simulation of the nucleation and growth of binary-alloy particles of Au, Ag, and Pd on NaCl(100) substrates

A. Schmidt, V. Schünemann, and R. Anton

*Institut für Angewandte Physik, Universität Hamburg, Jungiusstrasse 11,  
D-2000 Hamburg 36, Federal Republic of Germany*

(Received 8 November 1989; revised manuscript received 8 February 1990)

The initial phase of thin-film formation from two components that are simultaneously deposited on a substrate was simulated by Monte Carlo calculations of adatom processes, e.g., surface diffusion, reevaporation, nucleation, and cluster growth by collisions and capture. Experiments had revealed that the condensation of Pd is nearly complete on NaCl at 300°C, whereas Au and Ag exhibit very low initial condensation coefficients. Therefore, the composition of the nuclei differs strongly from that of the vapor beam. Monte Carlo calculations of the composition at the early stage of Au-Pd and of Ag-Pd depositions were fitted to experimental data from earlier work, which allowed us to determine the differences of the atomic energy parameters of the components, e.g., of the energies of adsorption  $E_a$  and of diffusion  $E_d$  with high accuracy. These differences are  $(E_a - E_d)_{Pd} - (E_a - E_d)_{Au} = 0.12 \pm 0.03$  eV, and  $(E_a - E_d)_{Pd} - (E_a - E_d)_{Ag} = 0.25 \pm 0.05$  eV.

### I. INTRODUCTION

In earlier work the heterogeneous condensation of binary-metal alloys, which were formed by simultaneous deposition of pure components, has been investigated.<sup>1-3</sup> The interpretation of the experimental results has been tried on the basis of an extended rate-equation system, which is well known for the case of a single component.<sup>4</sup> In this approach the population densities of adatoms adsorbed on the substrate surface, of nuclei, and of growing clusters are calculated from atomic-capture rates. Although such systems of differential equations are very complex, especially when dealing with more than one component, additional information about the condensation behavior of the components can be deduced from the development of the composition of the deposit, when the condensation of at least one component is incomplete. This is the case, for example, for Au and Ag on NaCl(100) cleavage surfaces,<sup>1</sup> whereas the condensation coefficient of Pd is near unity.<sup>5</sup> It has been pointed out in earlier work<sup>1</sup> that the difference of the composition of the initially formed particles from that of the vapor beam is a measure of a characteristic difference of atomic energy parameters, which is  $\delta E_{xy} = (E_a - E_d)_x - (E_a - E_d)_y$ , where  $E_a$  is the adatom adsorption energy,  $E_d$  the activation energy for surface diffusion on the substrate, and  $x$  and  $y$  denote the respective components.

However, accurate experimental determination of the composition of the particles has been difficult at early stages of formation, while the substrate coverage is small, due to the large error limits of the measurements<sup>1-3</sup> (see Sec. II). The question is how to extrapolate from data taken at later times with lower error margins to the beginning of the condensation.

A second problem arises when the condensation of at least one component is virtually complete, as is the case for Pd on NaCl(100), even at elevated temperatures. The

rate-equation approach will then only lead to analytical solutions by using rather rough approximations, since the adatom concentrations cannot be considered in a quasi-steady-state. The reason for this is that, since the nucleation density will be high, the adatom number densities will decrease more or less rapidly due to capture into growing particles. This will especially affect the component with a high condensation coefficient. However, even a low condensation coefficient, which would exhibit a quasi-steady-state of the adatom number density when deposited alone, may be influenced due to capture by clusters with a high number density, which are mainly produced by the other component. Numerical treatments of corresponding rate-equation systems are in progress and will be described in a forthcoming paper.<sup>6</sup>

One drawback of this approach is the fact that one only gets results of statistical significance but no direct information about the composition of the clusters. Their growth and composition can be described in a straightforward way by a diffusion model, which will be discussed in Sec. III. It will be shown that Monte Carlo simulations of adatom diffusion and capture are helpful in taking into account the influence of neighboring particles. Such calculations should give an answer to the question of whether large variations of the composition of different particles or of any particle with growth time may already occur at early stages. The aim of this work is to show that the Monte Carlo approach is well suited for this, and that the results allow fitting of experimental data and unambiguous extrapolation to the initial stages of condensation. From such fits, the above-mentioned differences of energy parameters can be deduced with high accuracy.

### II. EXPERIMENT

Binary-alloy particles of Pd-Au, Pd-Ag, and Au-Ag were deposited in ultrahigh vacuum by simultaneous eva-

poration of the components onto NaCl(100) surfaces, which had been obtained by cleavage *in situ*. In any case, the substrate temperature was kept constant at 300°C. Series of depositions were produced at constant vapor-beam fluxes of the components, but with increasing the deposition time in suitable steps. For the different series, the compositions of the vapor beam were changed. Each specimen was fixed *in situ* by overcoating with a thin carbon film, which was later floated off in water, and picked up onto a grid for transmission electron microscopy. For measurements of the composition of the deposits, we utilized energy-dispersive analysis of x rays (EDX) in a scanning electron microscope (SEM), with a special specimen holder for low background, which provides a very high sensitivity for thin-film analysis, which is comparable to Auger-electron spectroscopy. Nevertheless, for the early stages of deposition the deposited masses were often in the range of the detection limit. It should be noted that only the average composition of a large number of particles could be determined in any one specimen. Further details of the experimental procedures are described in earlier papers.<sup>1-3,5,6</sup>

### III. ADATOM PROCESSES AND MONTE CARLO SIMULATION

In this section a model for adatom diffusion and capture will be presented, and it will be shown that the composition of the growing particles can be calculated from the atomic-capture rates of the components. For this, an approximate analytical expression will be derived that takes into account adatom-depletion zones around growing clusters. Further, a Monte Carlo simulation of adatom processes will be presented, which allows one to calculate the composition of growing clusters without any need to specify certain adatom-depletion zones. In Sec. IV the results from analytical approximations will be compared with those from Monte Carlo calculations. Also, a fit of simulated to experimental data will be illustrated.

The basis of the diffusion model as well as of our Monte Carlo simulation is the "random walk" of adatoms on a substrate surface consisting of a square array of adsorption sites of distance  $a$ . The diffusion coefficients of atoms of type  $x$  or  $y$  are then given by<sup>7</sup>

$$D_{x(y)} = a^2 / (4\tau_0) \exp[-E_{dx(y)} / kT], \quad (1)$$

where  $E_{dx}$  and  $E_{dy}$  are atomic activation energies for surface diffusion,  $a$  is the length of a diffusion jump, and  $\tau_0^{-1}$  is the attempt frequency, which is generally assumed to be of the order of the Debye frequency, e.g., in the range  $10^{12}$ – $10^{13}$  s<sup>-1</sup>. In case of incomplete condensation, the mean residence times  $\tau$  of the adatoms on the surface before reevaporation are limited according to

$$\tau_{x(y)} = \tau_0 \exp[E_{ax(y)} / kT], \quad (2)$$

where  $E_{ax}$  and  $E_{ay}$  are the atomic adsorption energies on the substrate. The square root of the diffusion coefficient times the mean residence time, that is,

$$l_{x(y)} = \sqrt{D_{x(y)} \tau_{x(y)}}, \quad (3)$$

represents the adatom mean walk distances before reevaporation, which are determined by the differences  $(E_a - E_d)_{x(y)}$  at a given temperature. In accordance with earlier analyses of nucleation and growth experiments, diffusion of only monomers was assumed to occur. Dimers were considered stable nuclei, which do not dissociate and which are immobile on the substrate.

The adatom-capture probability as function of cluster size can be expressed as  $\sigma_n D_{x(y)}$ , where  $\sigma_n$  is a "capture number," representing a cross section, which depends on the cluster size. Usually, an adatom depletion, which is caused by the cluster acting as diffusion sink for adatoms, is incorporated into  $\sigma_n$  as follows:<sup>8</sup>

$$\sigma_n = (2\pi\mu) K_1(\mu) / K_0(\mu), \quad (4)$$

where  $K_i$  and  $K_0$  are modified Bessel functions of first and zeroth order, respectively, and  $\mu$  is a measure of the size of the particle, normalized to the adatom mean diffusion length  $l$ . (For a half-sphere with radius  $r$ ,  $\mu = r/l$ .) Thus,  $\sigma_n$  comes to depend on the sort of adatom being captured. The capture rates of atoms  $x$  (and  $y$ ) are then given by  $\sigma_n D_{x(y)} N_{x(y)}$ , and, neglecting direct impingement from the vapor beam, one obtains a differential equation for the particle growth rate with time:

$$\frac{d\mu}{dt} = (\Gamma\mu^2)^{-1} (v_x \sigma_{n,x} D_x n_x + v_y \sigma_{n,y} D_y N_y), \quad (5)$$

where  $\Gamma$  is a constant of geometry that depends on the three-dimensional shape of the particle, and  $v_x$  and  $v_y$  are the atomic volumes. (For a half-sphere,  $\Gamma = 2\pi$ .)

An analytical solution can be found by using the approximation  $(1/\mu) K_1(\mu) / K_0(\mu) \approx 1.265\mu^{-1.5}$  for small cluster sizes, and for the special case of quasicontant adatom concentrations  $N = R\tau$ . For an isolated cluster, one gets  $\mu = ct^{0.4}$  with constant  $c$ . The concentration  $c_x = n_x / (n_x + n_y)$  of atoms  $x$  in the particle is then easily calculated by integrating over the capture rates  $[=(\sigma D \tau R)_{x(y)}]$ :

$$c_x = [1 + (R_y / R_x) (l_y / l_x)^{1.5}]^{-1}, \quad (6)$$

with  $l_{x(y)} = \sqrt{D_{x(y)} \tau_{x(y)}}$ , according to Eq. (3). As expected, at steady state, and neglecting direct impingement, the composition of the particle stays constant. In general, however, the adatom concentrations are functions of time, as was discussed above. High particle number densities result in overlapping of capture zones, which leads to further reduction of the adatom populations, and, as a consequence, to a reduction of the particles' growth speed when compared to an isolated particle. Moreover, at later stages of growth, direct impingement of atoms from the vapor beam on the surfaces of the particles can no longer be neglected. By this effect, the composition of the particles will gradually approach that of the vapor beam.

The above considerations on the analytical expression for the capture-probability functions are presented here, because the results of this approximation will later be compared with Monte Carlo calculations, which will be

described in the following. The advantage of Monte Carlo simulation is that no assumption about depletion zones has to be made. Rather, such zones can, in principle, be deduced from such analyses. Also, the analytical solution only allows one to calculate the average composition of growing particles, whereas the Monte Carlo simulation allows one to calculate the compositions of individual clusters.

Calculations were performed on a square array of  $200 \times 200$  binding sites with distance  $a = 0.4$  nm. A frequency factor ( $\tau_0^{-1}$ ) of  $10^{12} \text{ s}^{-1}$  was assumed. After the adsorption of an adatom, the type of which being determined by a probability function given by the vapor-beam fluxes  $R_x$  and  $R_y$ , at a random site, the adsorption of another adatom was allowed. Subsequent hops of length  $a$  of both adatoms into randomly chosen directions eventually led to collision, thus forming a dimer, which was not allowed to move any more. Periodic boundary conditions were employed such that an adatom moving beyond the edge of the field reappeared at the opposite side. The hop probability was determined from Eq. (1), whereas reevaporation of adatoms was allowed according to a probability function derived from Eq. (2). In any case, complete accommodation of adatoms was assumed, e.g., the temperature in those equations was taken as that of the substrate. Collisions and capture of adatoms prevented further reevaporation, which means that the condensation coefficient of metal atoms on alloy clusters was assumed to be unity. This is justified, as all of our experiments done at a substrate temperature of  $300^\circ\text{C}$  so far have shown that the composition of the deposits asymptotically approaches that of the vapor beam at late stages of deposition, where the particle sizes and substrate coverages are large.

Direct impingement of atoms from the vapor beam on the surface of a growing cluster was taken into account as follows. If an adatom adsorption event occurred at the edge or on top of a cluster, this adatom was incorporated in it. Generally, for the early stages of particle growth as considered here, the number of directly impinging adatoms was much smaller, e.g., of the order of a few percent, than that of adatoms being captured by surface diffusion on the substrate.

At any instant the composition of any one cluster was calculated from the sum of the atoms of the components, which was incorporated up to that time of growth by surface diffusion and direct impingement.

Clusters formed by subsequent addition of adatoms by diffusion and direct impingement from the vapor beam were assumed to rearrange in pyramidlike shapes, as these were frequently observed in our deposits with Pd-Au and Pd-Ag particles. In the calculations the base planes were assumed to increase in steps of size equal to the distance of two adsorption sites, whenever the number of atoms exceeded the maximum number  $n$  of atoms, which can be placed in the volume of a pyramid with all edges of length  $D$ . The number  $n$  is related to  $D$  by  $n = 4D^3 / (3a_0^3\sqrt{2})$ , where  $a_0$  is the lattice constant of the fcc alloy particles. Here, a mean value of  $0.4$  nm was assumed. (In fact, the lattice parameter of the alloys considered here may vary between  $0.389$  and  $0.408$  nm.)

#### IV. RESULTS

All calculations were performed assuming a temperature of  $300^\circ\text{C}$ . The energies of adsorption and for surface diffusion were chosen as fit parameters such that experimental data for the early stages of deposition of Au-Pd and of Ag-Pd on NaCl(100) were closely matched. The main criterion was a close fit of compositions, as these depend very sensitively on differences of the energy values of the components. In addition to this, a second aim was to fit the absolute particle number densities, although the Monte Carlo approach is not well suited for this, because of the limited size of field.

Figure 1 illustrates the result of a Monte Carlo simulation for which a certain set of experimental parameters had been assumed, as given in the caption. Here, the calculated compositions of several individual clusters are plotted versus deposition time. Pd and Au were assumed to be deposited simultaneously with fixed vapor-beam fluxes. For the simulations the set of energy parameters, e.g.,  $E_a$  and  $E_d$ , was chosen to match experimental results for Au-Pd on NaCl(100) by trial and error (see below). The data points represent the composition history of the individual clusters, starting from the event of nucleation as a dimer, either pure or mixed. Most dimers consisted of two Pd atoms, or were mixed dimers, Au-Pd, and no dimer of the  $\text{Au}_2$  type occurred here. Reaching the "main sequence," e.g., the average composition of all clusters, the number of atoms in a cluster was about 20–30. After 9 s of growth the largest particles in this plot, e.g., those nucleated early, contain roughly 3,000 atoms. It is interesting to note that the compositions of the growing clusters, soon after nucleation, rapidly ap-

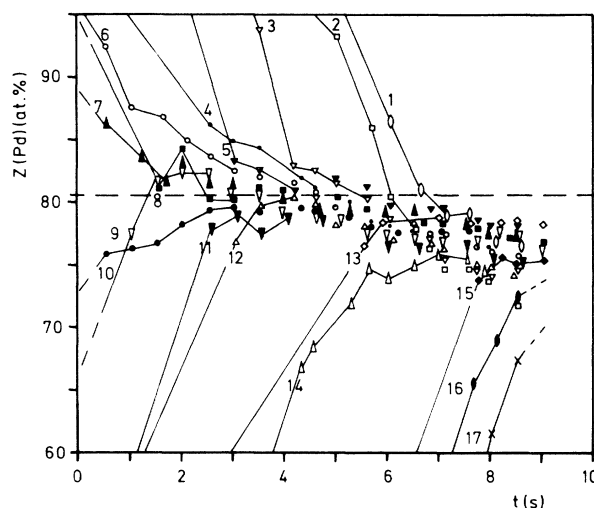


FIG. 1. The atomic concentration of Pd,  $Z(\text{Pd})$ , in 17 individual Pd-Au alloy particles on NaCl(100) vs deposition time, as calculated by Monte Carlo simulations. The assumed substrate temperature was  $300^\circ\text{C}$ , and the assumed vapor-beam fluxes were  $R_{\text{Pd}} = 1.77 \times 10^{13} \text{ cm}^{-2} \text{ s}^{-1}$  and  $R_{\text{Au}} = 2.53 \times 10^{13} \text{ cm}^{-2} \text{ s}^{-1}$ . The energy parameters were chosen as  $E_{a,\text{Pd}} = 0.78$ ,  $E_{d,\text{Pd}} = 0.33$ ,  $E_{a,\text{Au}} = 0.485$ , and  $E_{d,\text{Au}} = 0.155$  (all values in eV). The horizontal dashed line represents the composition as calculated from Eq. (6) (for further details, see text).

proach a mean value within statistical variations of a few percent. Moreover, for the early stages, this average value of about 80 at. % of Pd agrees well with that calculated from Eq. (6) to 81 at. %, as is indicated by the horizontal dashed line in Fig. 1. However, this composition differs strongly from that of the vapor beam, which is calculated from the flux rates of the components to about 41 at. % of Pd. The slight decrease with time of the concentration of Pd in the particles is not due to direct impingement, but is instead caused by the relatively high particle number density, which amounts to  $1 \times 10^{11} \text{ cm}^{-2}$  in this case. As pointed out above, neighboring clusters act as additional sinks for adatom diffusion. The capture zone around a cluster extends wider for that component with the longer mean adatom residence time on the substrate, which is Pd in this case. Overlapping of capture zones leads to a greater depletion of Pd than of Au adatoms. Thus, the fractional content of Au in the clusters may increase during growth. Without taking into account this different degree of adatom depletion of the components, the composition of the particles would be expected to stay constant, according to Eq. (6). This is also indicated by the horizontal dashed line in Fig. 1.

The fit of experimental data for Au-Pd on NaCl(100) at  $300^\circ\text{C}$  by Monte Carlo simulations is demonstrated in Fig. 2. Here, the development of the compositions with deposition time is plotted for four representative series with constant vapor-beam fluxes of the components, respectively. The compositions of the respective vapor beams (VB's) are marked at the right-hand scale. The Monte Carlo results extend from the start of deposition to up to 20 s, depending on the total number of clusters

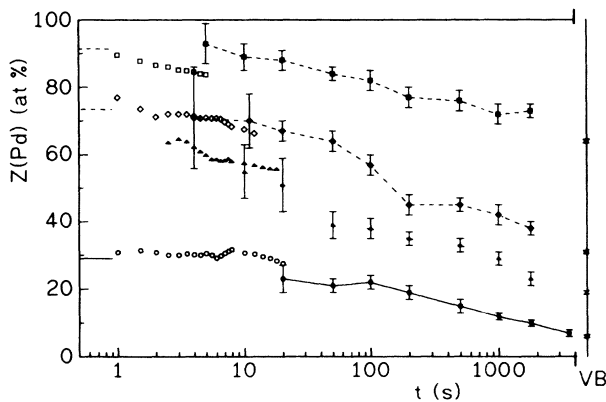


FIG. 2. Semilogarithmic plot of the atomic concentration  $Z(\text{Pd})$  of Pd in Pd-Au deposits on NaCl at  $300^\circ\text{C}$ , vs condensation time for four series at constant deposition rates of the components, respectively. The open symbols represent Monte Carlo results and the solid symbols with error bars are experimental data. For all series, the vapor-beam flux of Au was  $4.4 \times 10^{13} \text{ cm}^{-2} \text{ s}^{-1}$ , while that of Pd was varied: circles,  $R_{\text{Pd}} = 2.7 \times 10^{12} \text{ cm}^{-2} \text{ s}^{-1}$ ; triangles,  $1 \times 10^{13} \text{ cm}^{-2} \text{ s}^{-1}$ ; diamonds,  $2 \times 10^{13} \text{ cm}^{-2} \text{ s}^{-1}$ ; squares,  $7.9 \times 10^{13} \text{ cm}^{-2} \text{ s}^{-1}$ . For the Monte Carlo calculations the same energy parameters as given in Fig. 1 have been used. At the left-hand ordinate, the horizontal lines represent the initial compositions according to Eq. (6). The symbols at the right-hand ordinate mark the respective compositions of the vapor beams (VB's).

on the field in any one series, which limit the calculations in terms of CPU time. The four plots in Fig. 2 represent series with constant flux of Au, but with increasing flux of Pd from bottom to top, which means that the particle number density at a given time increases in the same direction. According to the argument given above, the calculated concentration of Pd is initially about constant for the series with lower vapor-beam fluxes of Pd,  $R_{\text{Pd}}$ , e.g., with relatively low particle number densities of below  $5 \times 10^{10} \text{ cm}^{-2}$  (see bottom plot in Fig. 2). The slight decrease with time seen in the other three series with larger  $R_{\text{Pd}}$  is due to the increased particle number densities of at or above  $1 \times 10^{11} \text{ cm}^{-2}$ . This behavior clearly demonstrates the effects of overlapping of capture zones around the clusters, as was discussed above. The subsequent relative decrease of the concentration of Pd, after deposition times above about 20 s, and the gradual approach to the composition of the corresponding vapor beam (as marked with VB at the right-hand ordinate in Fig. 2), is caused by the increasing effect of direct impingement, due to the increasing substrate coverage, as was explained in Sec. III.

The energy parameters were chosen by trial and error, such that all experimental data could be fitted using the same value of  $(E_a - E_d)_{\text{Pd}} - (E_a - E_d)_{\text{Au}} = 0.12 \text{ eV}$ . Use of this value to calculate the initial compositions from Eq. (6) also yielded reasonable agreement. From the quality of the fits, an error margin of  $\pm 0.03 \text{ eV}$  was estimated. A further criterion for the fit was the correspondence of calculated and observed particle number densities, as was mentioned above. In general, the nucleation density strongly depends on the absolute value of the atomic adsorption energy  $E_a$ , here of Pd, as Pd is the component with, by far, the highest condensation coefficient. Taking the energy parameters for Au from the work of Robins *et al.*,<sup>9</sup> namely  $E_a = 0.485 \text{ eV}$ ,  $E_d = 0.155 \text{ eV}$ , and  $(E_a - E_d)_{\text{Au}} = 0.33 \text{ eV}$ , we adjusted  $E_{a,\text{Pd}}$  and  $E_{d,\text{Pd}}$ , with constant difference  $(E_a - E_d)_{\text{Pd}} = 0.45 \text{ eV}$ , to fit calculated and experimentally measured particle number densities, which were in the range  $(3-10) \times 10^{10} \text{ cm}^{-2}$  at the early stages. A fair correspondence was achieved with  $E_{a,\text{Pd}} = 0.78 \text{ eV}$  and  $E_{d,\text{Pd}} = 0.33 \text{ eV}$ . Further discussion of the atomic-energy parameters will follow in Sec. V.

Results for Ag-Pd on NaCl at  $300^\circ\text{C}$  are plotted in Fig. 3. For three representative series of depositions, with constant vapor-beam fluxes of the components, respectively, the development of the concentration of Ag in the alloy deposits was followed by Monte Carlo calculations for up to about 20 s, while the experimental data continue up to 800 s of deposition time. As was already mentioned above, the initial condensation coefficient of Ag is very low, which implies large error margins in the experimental data in this regime. However, the general trend and the correspondence of the Monte Carlo data appear to be reasonable. For these calculations, the energy parameters of Pd were taken from the results of the Pd-Au experiments discussed above. As shown in Fig. 3, a good fit was obtained with  $\delta E_{\text{PdAg}} = (E_a - E_d)_{\text{Pd}} - (E_a - E_d)_{\text{Ag}} = 0.25 \text{ eV}$  within a possible variation of  $\pm 0.05 \text{ eV}$ . Here, the individual, absolute values of  $E_a = 0.4 \text{ eV}$

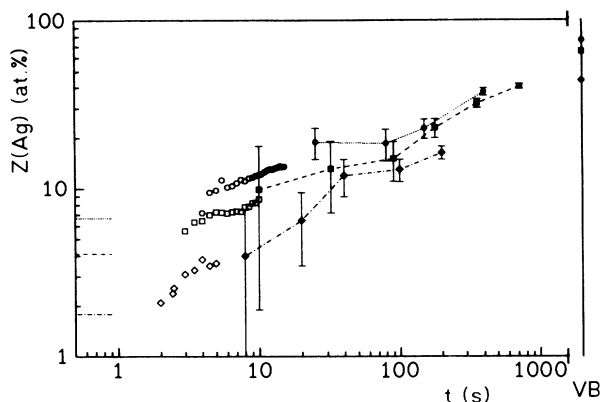


FIG. 3. Atomic concentration  $Z(\text{Ag})$  of Ag in Pd-Ag alloy deposits on NaCl(100) at  $300^\circ\text{C}$ , vs deposition time in double-logarithmic scaling. Monte Carlo results (open symbols) and experimental data (solid symbols) are plotted for three series with constant vapor-beam fluxes of the components. The flux of Ag was about the same for all cases:  $R_{\text{Ag}} = (2.8 \pm 0.2) \times 10^{13} \text{cm}^{-2} \text{s}^{-1}$ , while that of Pd was varied: circles  $R_{\text{Pd}} = 8.8 \times 10^{12} \text{cm}^{-2} \text{s}^{-1}$ ; squares,  $1.6 \times 10^{13} \text{cm}^{-2} \text{s}^{-1}$ ; diamonds  $3.4 \times 10^{13} \text{cm}^{-2} \text{s}^{-1}$ . For the Monte Carlo calculations the energy parameters of Pd were as given in Fig. 1. For Ag,  $E_{a,\text{Ag}} = 0.4$  and  $E_{d,\text{Ag}} = 0.2$  eV was chosen. As in Fig. 2, the horizontal lines at the left-hand ordinate represent the initial compositions as calculated from Eq. (6), whereas the symbols at the right-hand ordinate mark the compositions of the vapor beams (VB's), respectively.

and  $E_d = 0.2$  eV were chosen using arguments from other experimental findings, which will be discussed in the following section. It is interesting to note that with  $E_{a,\text{Pd}} = 0.78$  eV and  $E_{d,\text{Pd}} = 0.33$  eV, as for the case of Pd-Au, the calculated and experimental particle number densities were found to correspond reasonably well.

## V. DISCUSSION AND CONCLUSIONS

It is obvious that the initial composition of the alloy deposits—that is, is the nucleation phase—depends very sensitively on the difference  $\delta E_{xy} = (E_a - E_d)_x - (E_a - E_d)_y$  of the atomic-energy parameters of the components  $x$  and  $y$ . Variations with time during the early stages of deposition, where the role of direct impingement is not significant, may occur because of high particle number densities, as the particles act as sinks for diffusing adatoms. Of course, this effect depends on the absolute values of the atomic-energy parameters, as was discussed above. In our case, Pd exhibits the highest values, resulting in high particle number densities. The main aim of this work was to show that the differences of the energy parameters of the components in alloy deposits can be determined with relatively high accuracy by trial-and-error fits of Monte Carlo calculations to experimentally measured compositions at the early stages. However, such calculations require the knowledge of the individual, absolute energy values. The choice of these was led by several arguments from separate, previous experiments, as follows.

Recently, Gates and Robins<sup>9</sup> published energy data for Au on NaCl,  $E_a = 0.485$  eV, and  $E_d = 0.155$  eV that were based on a thorough discussion of experimental results from Velfe *et al.*,<sup>10</sup> which had been obtained under very-well-controlled conditions. This value of  $E_{a,\text{Au}}$  also corresponds to the upper limit of 0.5 eV, which had been determined by independent, atomic-scattering experiments.<sup>11</sup> Relying on these data, our result of  $(E_a - E_d)_{\text{Pd}} - (E_a - E_d)_{\text{Au}} = 0.12$  eV leads to  $(E_a - E_d)_{\text{Pd}} = 0.45$  eV. Keeping this difference constant, we adjusted  $E_{a,\text{Pd}}$  to 0.78 eV in order to match calculated particle number densities with experimental ones, which resulted in  $E_{d,\text{Pd}} = 0.33$  eV. These values also seem to be supported by the close fit of particle number densities for the case of Pd-Ag alloy deposits, obtained with the same value of  $E_{a,\text{Pd}}$ , where the lower-energy parameters of Ag are of no influence (see below).

In earlier work on Au-Ag depositions on NaCl,<sup>1</sup> the differences  $E_{a,\text{Au}} - E_{a,\text{Ag}} = 0.08$  eV and  $E_{d,\text{Au}} - E_{d,\text{Ag}} = -0.03$  eV had been derived from measurements of the composition in the steady-state regime of nucleation, which in that case extended well into the experimentally accessible regime of deposition time because of initially rather incomplete condensation of both components. Furthermore, atomic-beam-scattering experiments with Ag from NaCl surfaces had revealed an upper limit for  $E_{a,\text{Ag}}$  of 0.5 eV.<sup>12</sup> Thus, we would obtain  $E_{a,\text{Ag}} = 0.405$  eV and  $E_{d,\text{Ag}} = 0.185$  eV, with  $(E_a - E_d)_{\text{Ag}} = 0.22$  eV, which are close to the values 0.4, 0.2, and 0.2 eV, respectively, used in our Monte Carlo fits.

A third argument comes from the previously cited experiments with Au-Ag alloys on NaCl,<sup>1</sup> which resulted in  $\delta E_{\text{AuAg}} = (E_a - E_d)_{\text{Au}} - (E_a - E_d)_{\text{Ag}} = 0.11$  eV. In fact, this value agrees with our results from Monte Carlo fits to experimental data, e.g.,  $\delta E_{\text{PdAu}} = 0.12 \pm 0.03$  eV and  $\delta E_{\text{AgPd}} = -0.25 \pm 0.05$  eV, in the sense that the sum of all three values should be zero, which is the case within the error limits. This means that the set of energy parameters is consistent, with no contradictions. In particular, it means that the adatom mean walk distance before reevaporation according to Eq. (3) is roughly 3 times larger for Au than for Ag, whereas it is about 10 times larger for Pd than for Ag, on NaCl(100) at  $300^\circ\text{C}$ . It should be noted, however, that the error in the individual, absolute energy values of Pd and Ag may be of the order of 0.1 eV whereas the differences  $\delta E_{xy}$ , which are derived from fits of the composition alone, appear to be rather accurate and reliable.

In conclusion, our Monte Carlo simulations of the nucleation and growth of alloy clusters have revealed that close fits, especially of the initial composition, can be achieved on rather simple premises, e.g., that only monomers are mobile on the substrate and that dimers are stable nuclei, which, like larger clusters, do not diffuse. Although there are indications from other experimental data that the mobility of clusters may play a major role, especially regarding the nucleation density, such effects are considered to be of minor importance here, as mainly the later development of the composition of the clusters will be affected. Also, the role of defects on the alkali halide surface, which had been discussed in the litera-

ture,<sup>8,9</sup> originating from charged particles, and acting as nucleation centers, does not influence the composition of the clusters during the early stages of growth in a first approximation, as long as the nucleation densities are not

too high, as was discussed above. Therefore, we consider the differences of the energy parameters, and especially of the ratios of the adatom mean walk distances of the components given above, as being fairly reliable.

---

<sup>1</sup>R. Anton, M. Harsdorff, and Th. Martens, *Thin Solid Films* **57**, 233 (1979).

<sup>2</sup>R. Anton and R. Dröske, *Thin Solid Films* **124**, 155 (1985).

<sup>3</sup>T. Kortekamp, R. Anton, and M. Harsdorff, *Thin Solid Films* **145**, 123 (1986).

<sup>4</sup>See, for example, J. A. Venables, G. D. T. Spiller, and M. Hanbücken, *Rep. Prog. Phys.* **47**, 399 (1984).

<sup>5</sup>A. Schmidt, M. Spode, J. Heinrich, and R. Anton, *Thin Solid Films* (to be published).

<sup>6</sup>R. Anton, A. Schmidt, and V. Schünemann, *Vacuum* (to be published).

<sup>7</sup>B. Lewis and G. J. Rees, *Philos. Mag.* **20**, 1253 (1974).

<sup>8</sup>B. Lewis and J. C. Anderson, *Nucleation and Growth of Thin Films* (Academic, New York, 1978), 73.

<sup>9</sup>A. D. Gates and J. L. Robins, *Thin Solid Films* **149**, 113 (1987).

<sup>10</sup>H. D. Velfe, H. Stenzel, and M. Krohn, *Thin Solid Films* **98**, 115 (1982).

<sup>11</sup>E. -A. Knabbe and M. Harsdorff, *Thin Solid Films* **57**, 271 (1979).

<sup>12</sup>R. Anton, R. Behling, M. Harsdorff, and Chr. Kleinschmidt, *Thin Solid Films* **140**, 291 (1986).